

# Grey Wolf Optimized PNN for the Detection of Faults in Induction Motors

N. Sivaraj<sup>1,\*</sup>, B. Rajagopal<sup>2</sup>

Submitted: 10/09/2022

Accepted: 20/12/2022

**Abstract:** Induction motors, commonly referred as asynchronous machines, are the most frequently used electrical machinery in industries. The induction motor (IM) plays a crucial role in many industrial applications in the current world because of its many advantages, including its low cost, sturdy nature, etc. There are a variety of causes for induction motor defects, including overcurrent, undercurrents, starter problems, overvoltage, overloading, motor overheating, etc. Therefore, it is crucial to defend the motor from errors. The objective of this study is to use Grey Wolf Optimized PNN is used to find induction motor defects. In this paper some of the processing operations like Filtering, segmenting, extracting and classifying were carried out on the driven motor's retrieved output signals. The proposed method combines the wiener filter for pre-processing, the Gabor wavelet transform for segmentation, the Grey-Level Co-Occurrence Matrix for extracting features and the Grey Wolf Optimized PNN for classification.

**Keywords:** Induction Motor, Grey Wolf Optimized PNN, Wiener Filter, Grey-Level Co-Occurrence Matrix.

## 1. Introduction

Induction Motors (IM) are the most broadly utilized electromechanical conversion devices in the world. Currently, it is used for all manufacturing applications and meets around two thirds of all commercial electricity demands. Therefore, it is crucial to establish effective methods for defect identification in induction motors [1]. Now there are more and more three phase IM applications being used in industrial and commercial settings [2]. Various speeds are required by many industrial applications to manage various loads. The speed of an IM can be easily modified and IMs are available in a variety of torque and speed levels. Since IMs are more durable than DC motors, they are employed in a variety of climatic conditions that other motors cannot handle [3]. However, IM frequently has sudden failures as a result of rotor and bearing faults. If a bearing failure occurs in an IM and it is not detected at an earlier time, the machine will suffer serious harm [4]. For the drive of three-phase induction motors, sensor-less direct vector control approaches are frequently used. These control strategies are used to estimate the rotor flux, rotor speed, and load torque of the two motors [5].

The primary areas of interest are high-precision torque estimation and control of induction motor drives owing to the extensive use of induction motors in torque-controlled applications, such as electric vehicles. Accurate flux estimation and motor model estimates have a considerable impact on the open-loop torque control's performance [6]. For the purpose of diagnosing stator faults, power signature analyses are either directly or indirectly performed and a running three-phase induction motor with a squirrel cage is connected. An active and reactive power medium coupling, along with the stator voltage modulus, makes it simple to distinguish between the stator fault circumstances and other irregularities [7]. For the purpose of controlling the motor's speed and rotor flux, a static converter supplies the stator windings. A novel method for stator faults detection in induction motors fed by inverters under closed-loop control is proposed in [8]. Stator current components or an increase in amplitude of specific components at particular frequencies are indicators of a motor fault state. Induction motors can detect mechanical and electrical problems using the well-tested method known as motor current signature analysis. However, the amplitude of these components rises when a fault is present and is very low for healthy devices [9].

The performance of the fault tolerant three phase induction motor drives now available has been impacted by the current and voltage constraints for the inverter and

<sup>1</sup>Research Scholar, Department of Electrical Engineering, Annamalai University, Chidambaram, Tamil Nadu, India.

<sup>2</sup>Associate Professor, Department of Electrical Engineering, Annamalai University, Chidambaram, Tamil Nadu India.

\*Corresponding Author Email: sivarajn213@gmail.com

machine. Due to the absence of consideration for the flux producing current, this technique does not accurately require the torque in post fault mode. Due to this, the motor's top speed in post fault mode is impacted, which in turn affects a massive post fault power [10]. Early identification of IM faults utilising an electric current signal is performed by a Spectral Synch (SS) method. The developed SS method's efficiency is revealed on IMs with damaged bearings and IMs with broken rotor bars [11]. Due to the potential financial losses that unexpected failures of these equipment might cause for the respective businesses, condition monitoring of the motors is of highest concern. To address the drawbacks of induction motors, for the first time in soft started induction motors, a significant validation of a rotor problem diagnosis method is used [12]. One of the crucial electrical defects that impacts the dependability of numerous industrial applications in an induction motors is an Inter Turn Short Circuit (ITSC) fault. Robustness is the main obstacle to using these methods to uncover ITSC flaws, despite the fact that there is a lot of interest in their application [13]. Due to the Broken Rotor Bar (BRB) frequencies components create low impact and proximity to the supplying input frequency and it is difficult to identify the stator current. So Recursive Undecimated Wavelet Packet Transform (RUWPT) method is used to remove one parameter that can detect the problem in arbitrary working conditions and for low load cases in order to tackle this limitation [14]. Empirical Mode Decomposition (EMD) is suggested as a reliable method for detecting broken bars defects in industrial induction motors with line-start and inverter fed [15].

Currently, induction motor defect detection by using neural networks is a common practise. The primary issues with induction motors are escalating costs, worsening working conditions and quality production. Support Vector Machines (SVMs) is used to detect faults in induction motors. Artificial Neural Network and the Fuzzy Logic (FL) were used to compare the SVM procedure with another two artificial intelligence methods (ANN). The SVM is less dependent on several factors than the ANN, which affects the proportion of accurate detections [16]. In order to examine the frame vibrations during start-up, Continuous Wavelet Transform (CWT), a strong signal-processing tool is combined with support vector machine (SVM) [17]. The defective motor is examined by Correlation and Fitness Values based Feature Selection (CFFS). The drawback of CFFS is greater running expenses for other purposes with high-dimensional characteristics [18]. Early stator defect detection is crucial since they spread quickly and could result in additional motor damage [19]. Direct Torque Control (DTC) uses stator resistance of the machine to calculate the stator flux. It is a reliable and efficient

indicator that an artificial neural network uses to detect and diagnose stator turn issues [20].

To overcome these issues the Probabilistic neural network (PNN) is employed, which discovers the fault in induction motor. This study introduces Grey Wolf Optimized PNN for detection of faults in induction motors which includes wiener filter for pre-processing, Gabor wavelet transform for segmentation, for feature extraction GLCM and Grey Wolf Optimized PNN for classification.

## 2. Description of the Proposed Work

Power electronics have obviously become more accessible and have developed on a worldwide scale. To implement a single phase motor drive, however, a more straightforward approach is workable in a number of applications. For driving rectifiers, DC motor systems, and industrial machinery requires an induction motors respectively. However, because of the rotor and bearing issues, IM frequently have an unexpected failures. As a result, IM errors must be identified by a fault detection system. Fig. 1 provides an illustration of the proposed work's description.

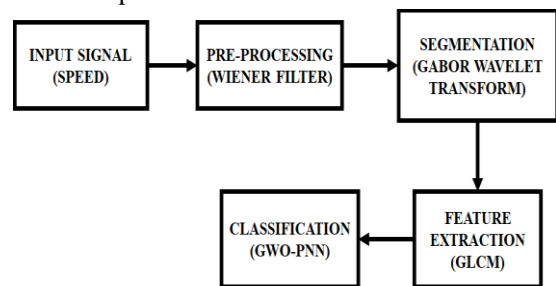


Fig. 1: Proposed work

To prevent unanticipated damage in industrial processes, fault detection in an induction motor, especially at an early stage, has become essential. So in order to manage the speed of a single phase induction motor, a control technique is used. In pre-processing method, the Wiener filter's noise cancellation technique is used to evaluate the fault severity from stator current. In the process of segmentation Gabor wavelets transformations are employed to maximize the theoretical limit of joint resolution between space and frequency domain. Statistical texture features of second order can be extracted by using the GLCM approach in feature extraction. In order to achieve optimal PNN training parameter settings and a high level of accuracy, the GWO technique is adopted for classification.

### 2.1. Wiener filter

The Wiener filter employs spectral analysis to separate the desired data from noise while recognizing both as stochastic processes with linear features. WK coefficients

are used to apply this linear filter to a valued signal. Noise is present in the input signal  $x(n)$ .

$$x(n) = d(n) + v(n) \quad (1)$$

An output signal  $y(n)$ , ought to be a reasonable approximation of  $d(n)$ . Thus,  $e(n)$  is the lowest error signal. In order to reduce a mean square error, an adaptive algorithm rectifies the weights  $W_k$ .

$$e = \min (E(e(n)^2)) \quad (2)$$

$$e(n) = y(n) - d(n) \quad (3)$$

The following equation is used by a  $k$  tap discrete Wiener filter to determine  $y$ 's value ( $n$ ).

$$y(n) = \sum_{k=0}^{N-1} W_k(d(n-k) * v(n-k)) \quad (4)$$

The most important characteristic of the Wiener filter is the Wiener-Hopf equation, which determines the ideal weights.

$$\sum_{i=0}^{p-1} w_{0|r_{xx}}(k-1) = r_{xd}(-l) \quad (5)$$

Where the ideal tap weight values for the filter are  $W_0, W_1, \dots$  and  $W_{p-1}$ . An autocorrelation function of  $x(n)$  is denoted by  $r_{xx}$ . A cross correlation function between  $x(n)$  and  $d(n)$  is  $r_{xd}$ . The Wiener filter block diagram is clearly displayed in Fig. 2.

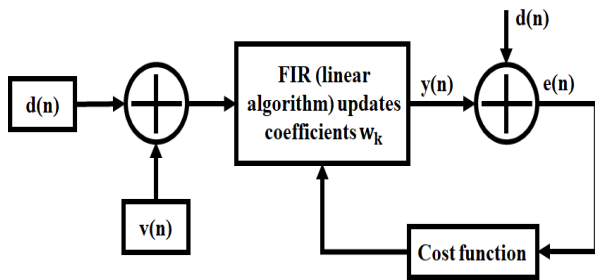


Fig. 2: Block diagram of Wiener filter

## 2.2. Gabor Wavelet Transform (GWT)

The human visual process is modelled as a filter bank by Gabor functions with various orientations and frequencies. To generate a Gabor wavelet, a Gaussian kernel function can be modified by using a sinusoidal plane wave that has the optimum position in both the space domain and the frequency domain. The literature defines a wide range of computer vision applications using Gabor functions, including signal processing, discriminations, and texture segmentation. While offering a fine adjustment for frequency attributes, Gabor wavelets highlight the directional characteristics of a signal. The ability to alter frequency is especially crucial for reducing background noise in medical signals. The most crucial aspect of the noise reduction technique is the retention of the edge's characteristics. The following is a definition of a 2D Gabor wavelet:

$$G(x, y, \theta, u, \sigma) = \frac{1}{2\pi\sigma^2} \exp\left\{-\frac{x^2+y^2}{2\sigma^2}\right\} \exp\{2\pi j(ux \cos \theta + uy \sin \theta)\} \quad (6)$$

Where, the orientation of the wave is mentioned as  $\theta$ , the frequency of the sinusoidal wave is mentioned as  $u$ , a

standard deviation of the Gaussian function in the  $x$  and  $y$  direction and  $j = \sqrt{-1}$  is mentioned as  $\sigma$ . The result of a Gabor filtering can be represented as a 2D convolution of the input signal  $(x, y)$  and  $(x, y)$ . Due to the complexity of the Gabor wavelet, the outcome is a 2D complex signal. An absolute of this signal is one that keeps the edge's features.

When the wave vector is perpendicular to the edge, the Gabor wavelets strengthen an edge and remove background information. Local characteristics in the convolutional result signal point to the signal's edge. By adjusting the orientation factor, one can obtain kernels associated with angles. The Gabor wavelet is essentially a complex wavelet with a few notable frequency parameter oscillations. Depending on the value of, the oscillations' magnitude decay rate changes. Due to the characteristics of the 2D Gabor wavelet, it is particularly useful for extracting the waveform and directional features that are appropriate for keeping edge pixels while suppressing noise, which is prevalent in medical signals.

## 2.3. GLCM features

The time-frequency content is described by using texture analysis techniques. To determine the content of a signal, a number of texture-based techniques were developed, comprising the autocorrelation function (ACF), the binary Gabor pattern (BGP), the local binary pattern (LBP), the local spiking pattern (LSP) and the gray-level co-occurrence matrix (GLCM). After figuring GLCM for  $k$ th channel of speed signal, i.e.  $G_k$ , with  $L$  levels, features like entropy ( $S$ ) and energy ( $e_k$ ), which are calculated as follows:

According to equation 7, energy is the degree of the pair's concentration at a certain grey intensity on the co-occurrence matrix.

$$Energy = \sum_{i=1}^L \sum_{j=1}^L p(i, j)^2 \quad (7)$$

Entropy displays an unpredictable nature of the shape and size. In addition to calculating signal information, which is specified in equation 8, entropy also quantifies information or messages lost from transition signals.

$$Entropy = \sum_{i=1}^L \sum_{j=1}^L p(i, j)(- \ln p(i, j)) \quad (8)$$

The GLCM can be used to illustrate various combinations of grey levels within the signal, which can be helpful in identifying the various areas of interest in the signal. The second-order link between the neighbouring pixels and references are taken into consideration when GLCM extracts the relevant features.

## 2.4. GWO algorithm

Hunting techniques and social management are employed by grey wolves in nature are modelled by GWO algorithm. In addition to using it to solve optimisation issues, the researchers employed mathematical modelling to illustrate the main phases of the wolf's hunting process. GWO algorithm is shown in Fig. 3.

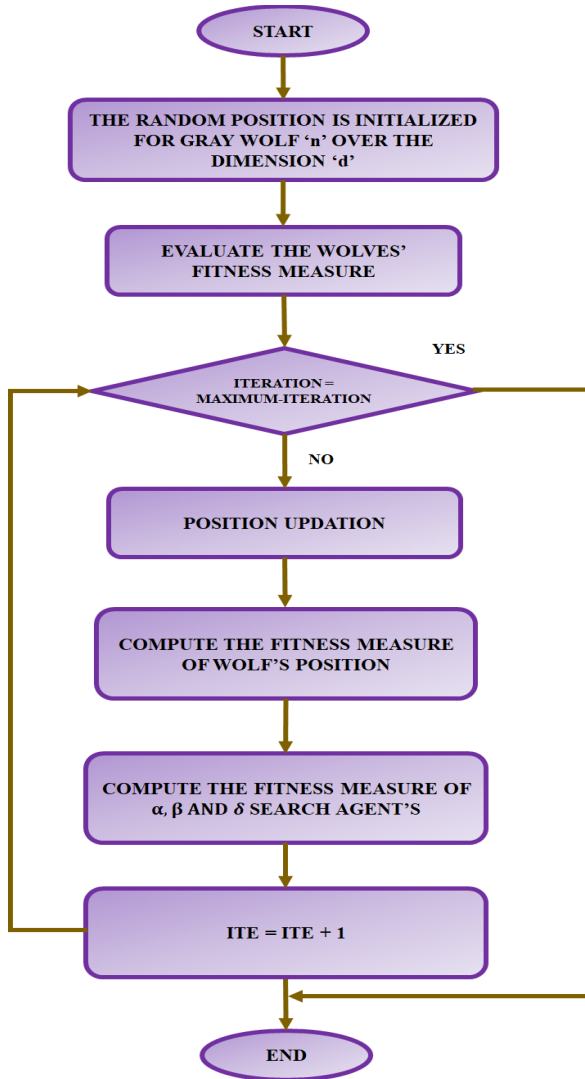


Fig. 3: GWO Algorithm

Alpha ( $\alpha$ ), beta ( $\beta$ ), delta ( $\delta$ ) and omega ( $\omega$ ) are four groups in the GWO algorithm population. Three wolves that were determined to have the best parameter fit were  $\alpha$ ,  $\beta$ , and  $\delta$ . They directed another wolves that were still present ( $\omega$ ) to the favourable locations within a search space. The wolves circled their victim while they were maximising, and the following mathematical equations can be used to describe this behaviour:

$$\vec{D} = |\vec{C} \cdot \vec{X}_p(t) - \vec{X}(t)| \quad (9)$$

$$\vec{X}(t + 1) = \vec{X}_p(t) - \vec{A} \cdot \vec{D} \quad (10)$$

Where the coefficient vectors are represented as  $\vec{A}$  and  $\vec{C}$ ,  $\vec{X}_p$  labels a position vector of the prey as  $\vec{X}_p$  and a position vector of grey wolf as  $\vec{X}$ .  $\vec{C}$  and  $\vec{A}$  vectors are calculated as follows:  $\alpha$ ,  $\beta$ , and  $\delta$

$$\vec{A} = 2 \cdot \vec{a} \cdot r1 - \vec{a} \quad (11)$$

$$\vec{C} = 2 \cdot r2, (4) \quad (12)$$

Where  $r1, r2$  are the random vectors utilised in  $[0, 1]$  and the components are linearly dropped to 0 from 2 by using a few iterations. The grey wolf may update its position using the above equations if the prey were to move from position  $(X, Y)$  to position  $(X^*, Y^*)$ . Several positions that are closer to the best agent than the current location could be achieved by adjusting the values of the  $A$  and  $C$

vectors. As an illustration,  $(X^*, X, Y^*)$  is obtained by determining that  $\vec{A} = (1, 0)$  and  $C = (1, 1)$ . The grey wolves can reach any spot that is present between the random vectors  $r1$  and  $r2$ , it must be highlighted. As a result, the wolf may randomly update its location within the area surrounding the prey using the equations above. The placements of the prey are suggested by the GWO approach to be  $\alpha, \beta$  and the initial three best solutions are taken to be  $\alpha, \beta$ , and  $\delta$  during an optimisation process. The following is a description of the calculated model that signifies the repositioning of the wolves:

$$\vec{D}\alpha = |\vec{C}1 \cdot \vec{X}\alpha - \vec{X}| \quad (13)$$

$$\vec{D}\beta = |\vec{C}2 \cdot \vec{X}\beta - \vec{X}| \quad (14)$$

$$\vec{D}\delta = |\vec{C}3 \cdot \vec{X}\delta - \vec{X}| \quad (15)$$

Where  $X\beta$  denotes the  $\beta$  position,  $\vec{X}\delta$  labels the  $\delta$  position and  $\vec{X}\alpha$  denotes the  $\alpha$  position. The random vectors are  $\vec{C}1, \vec{C}2, \vec{C}3$ , while  $\vec{X}$  shows a position used in this solution. The step size of the wolf approaching the wolves is clearly specified, as illustrated in Eqs. (13), (14) and (15). Using the existing solution, the predicted end positions of the wolves are as follows:

$$\vec{X}1 = \vec{X}\alpha - \vec{A}1 \cdot (\vec{D}\alpha) \quad (16)$$

$$\vec{X}2 = \vec{X}\beta - \vec{A}2 \cdot (\vec{D}\beta) \quad (17)$$

$$\vec{X}3 = \vec{X}\delta - \vec{A}3 \cdot (\vec{D}\delta) \quad (18)$$

$$\vec{X}(t + 1) = \frac{\vec{X}1 + \vec{X}2 + \vec{X}3}{3} \quad (19)$$

Where a positions of  $\alpha, \beta$ , and  $\delta$  wolves are mentioned as  $X\alpha, X\beta$  and  $X\delta$ , respectively. The random vectors are  $\vec{A}1, \vec{A}2, \vec{A}3$ , while  $t$  represents total number of iterations. The final location of the wolves is established, as indicated in Eqs. (16), (17), (18) and (19).

#### 2.4.1. Proposed GWO-PNN

There are two hidden layers and one input layer in a PNN. The pattern units are contained in the first hidden layer. The back-propagation NN approach is different from the PNN approach. The PNN's main benefit is that the probabilistic technique just requires one learning step. Backward propagation NN learning is comparable to learning via trial and error. Contrarily, the PNN gains knowledge from experience rather than through trial and error.

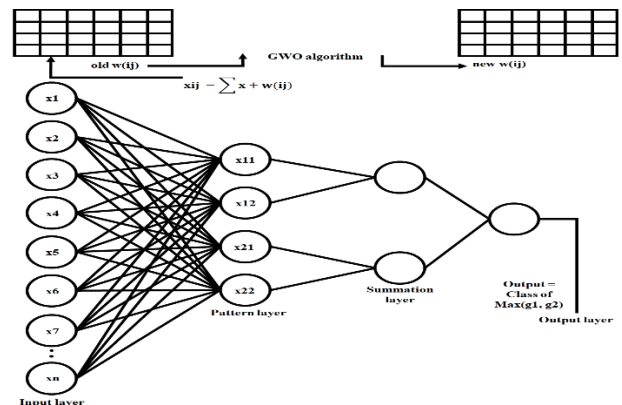


Fig. 4: Mechanism of GWO Algorithm with PNN.

A PNN has a strong framework and exceptionally viable operations. Even with a limited amount of training instances, it still performs effectively. The proper weights  $w(ij)$ , which are calculated using the PNN approach and shown in Fig. 4, are multiplied by the output of this input dataset. Then transferred to the pattern layer. A transfer function is used to transform them into the summation and output layers, as it was previously demonstrated. The output layer, which is the final layer, normally consist of one class because only one output is required. The main objective of the training process is to identify the most precise weights that were assigned to a connector line. The GWO technique was chosen in order to obtain optimised PNN training parameter settings and to achieve a high level of accuracy.

### 3. Result and Discussion

In this work fault detected in induction motor using an optimized neural network approach. Basic signal processing concepts are applied for an efficient and accurately detected the faults. The obtained simulation outputs are presented and explained below as follows:

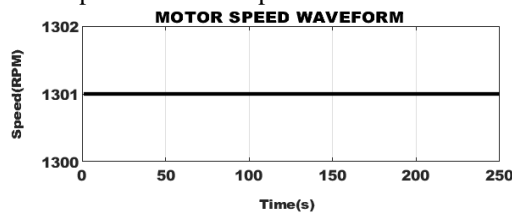


Fig. 5: Motor speed waveform

Fig. 5 displays the speed waveform of the motor which indicates a constant speed value of 1301 RPM. This speed signal is applied as the input to the Wiener filter for the efficient preprocessing approach.

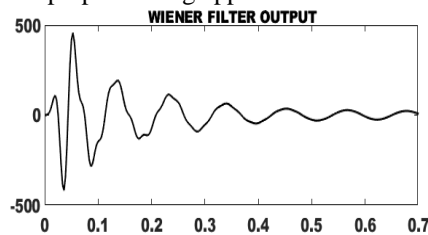


Fig. 6: Wiener filter output

A wiener filter is a tool used in signal processing that removes undesirable elements or features from a signal. Signal to noise ratios are optimized with the Wiener filter and the obtained output is clearly shown in Fig. 6.

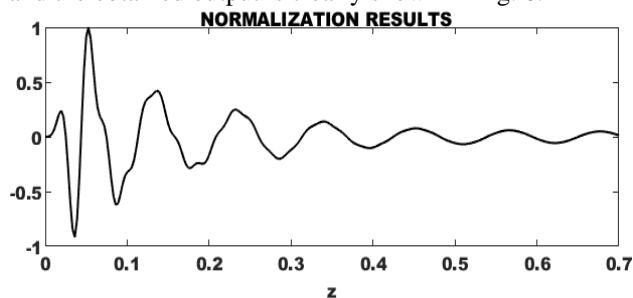


Fig. 7: Normalization results

Normalization makes a signal's amplitude correspond to a particular standard. Fig. 7, shows a histogram with a normalised frequency distribution with a range of the normalized frequency is  $[0, 0.7]$ .

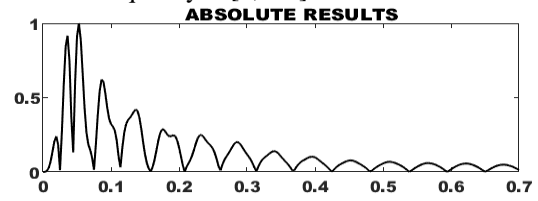


Fig. 8: Absolute results

Fig. 8, clearly shows the frequency range of an absolute of the proposed work respectively.

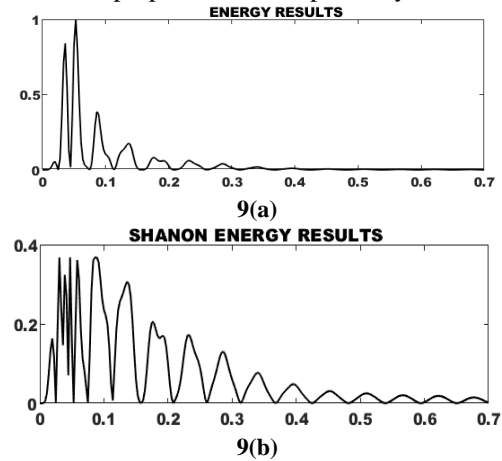


Fig. 9(a) Energy results 9(b) Shanon energy results

In order to improve significant peaks for reliable peak detection, Shannon energy has been integrated into peak detection methods of various signals is clearly shown in Fig.: 9(a, b).

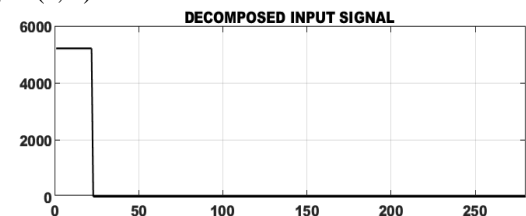
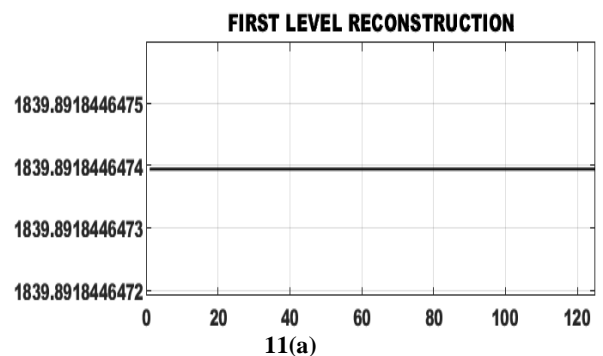


Fig. 10: Decomposed input signal

Decomposition, which involves splitting a single signal into two or more additive components, is the opposite of synthesis.



11(a)

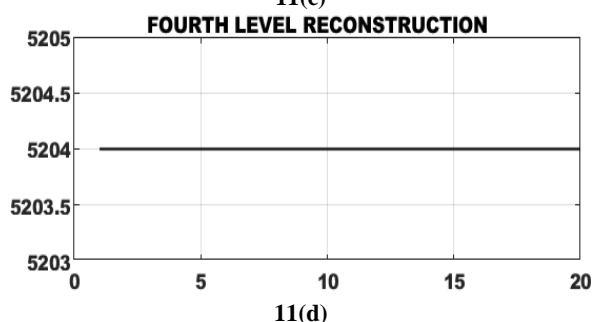
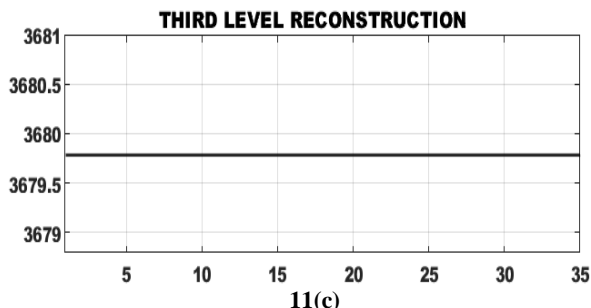
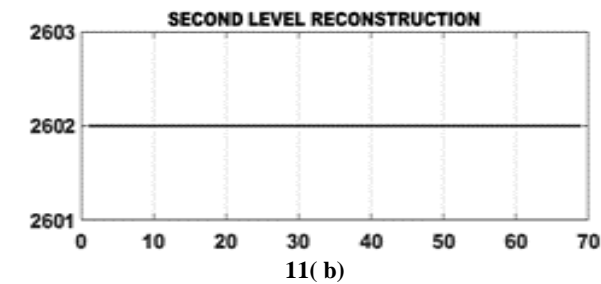


Fig. 11(a) (b) (c) (d): First, second, third and fourth level reconstruction

Fig. 11 (a), (b), (c) and (d) illustrates this process as the first, second, third and fourth levels of reconstruction, which are comparable to interpolating between points on a graph. However, it can be demonstrated that, under certain circumstances, an original analogue signal may be precisely recreated from its samples.

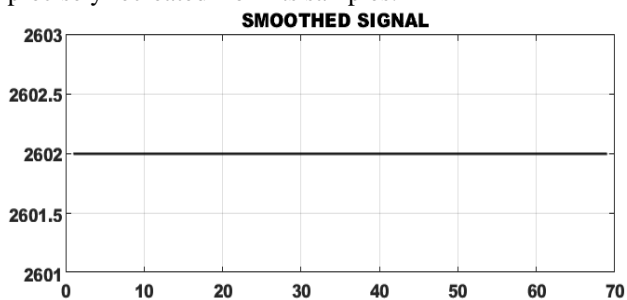


Fig. 12: Smoothed signal

The smoothing of a signal is vividly illustrated in Fig. 12 by a function that creates important patterns in the signal respectively.

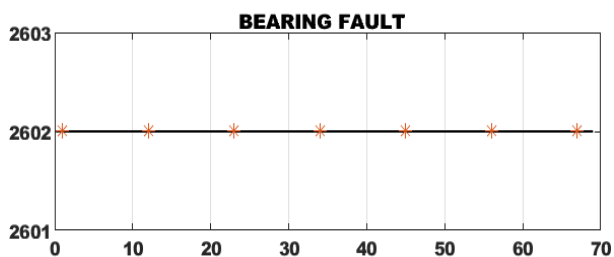


Fig. 13: Bearing fault

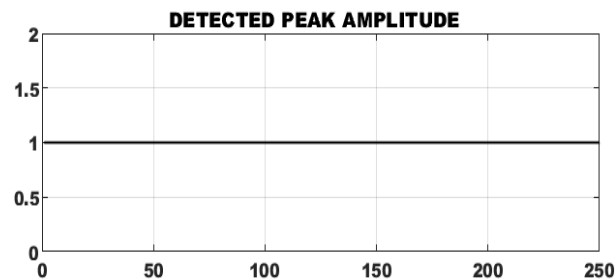


Fig. 14: Detected peak amplitude

Fig. 13, indicates the bearing faults in an induction motors by adopting signal processing approach. The detected peak amplitude is indicated in Fig. 14.

#### 4. Conclusion

Nowadays, the induction motor (IM) is an essential component in a variety of industrial applications, because of its many advantages, such as its cost and durability. Induction motor flaws are to be found using the Grey Wolf Optimized PNN in this study. The driven motor's retrieved output signals were subjected to some processing procedures in this study, including filtering, segmenting, extracting, and classifying. The suggested approach combines feature extraction using the Grey Level Co-Occurrence Matrix (GLCM), segmentation using the Gabor wavelet transform and classification using the Grey Wolf Optimized PNN.

#### References

- [1] Guerra de Araujo Cruz A., Delgado Gomes R., Antonio Belo F., Cavalcante Lima Filho A., *A Hybrid System Based on Fuzzy Logic to Failure Diagnosis in Induction Motors*, in IEEE Latin America Transactions, 2017, **15**(8), p.1480-1489.
- [2] Ferreira, Fernando JTE, Ge Baoming, de Almeida A. T., *Reliability and Operation of High-Efficiency Induction Motors*, in IEEE Transactions on Industry Applications, 2016, **52**(6), p. 4628-4637.
- [3] Ojaghi M., Akhondi R., *Modeling Induction Motors Under Mixed Radial-Axial Asymmetry of the Air Gap Produced by Oil-Whirl Fault in a Sleeve Bearing*, in IEEE Transactions on Magnetics, 2018, **54**(11), p. 1-5.
- [4] Malla, S., M. J. . Meena, O. . Reddy. R, V. . Mahalakshmi, and A. . Balobaid. "A Study on Fish Classification Techniques Using Convolutional Neural Networks on Highly Challenged Underwater Images". International Journal on Recent and Innovation Trends in Computing and Communication, vol. 10, no. 4, Apr. 2022, pp. 01-09, doi:10.17762/ijritcc.v10i4.5524.
- [5] Pandarakone S.E., Mizuno Y., Nakamura H., *Distinct Fault Analysis of Induction Motor Bearing Using Frequency Spectrum Determination and Support Vector Machine*, in IEEE Transactions on Industry Applications, 2017, **53**(3), p. 3049-3056.
- [6] Gunabalan R., Sanjeevikumar P., Blaabjerg F., Ojo O., Subbiah V., *Analysis and Implementation of Parallel Connected Two-Induction Motor Single-Inverter Drive by Direct Vector Control for Industrial Application*, IEEE

- Transactions on Power Electronics, 2015, 30(12), p. 6472-6475.
- [7] Gupta, D. J. . (2022). A Study on Various Cloud Computing Technologies, Implementation Process, Categories and Application Use in Organisation. International Journal on Future Revolution in Computer Science & Communication Engineering, 8(1), 09–12. <https://doi.org/10.17762/ijfrcsce.v8i1.2064>
- [8] Stender M., Wallscheid O., J. Bocker, " Senior Member, *Accurate Torque Control for Induction Motors by Utilizing a Globally Optimized Flux Observer*, IEEE Transactions on Power Electronics, 2021, 36(11), p. 13261-13274.
- [9] Drif M., Cardoso A.J.M., *Stator Fault Diagnostics in Squirrel Cage Three-Phase Induction Motor Drives Using the Instantaneous Active and Reactive Power Signature Analyses*, IEEE Transactions on Industrial Informatics, 2014, 10(2), p. 1348-1360.
- [10] Elbouchikhi E., Amirat Y., Feld G., Benbouzid M., *Generalized Likelihood Ratio Test Based Approach for Stator-Fault Detection in a PWM Inverter-Fed Induction Motor Drive*, IEEE Transactions on Industrial Electronics, 2019, 66(8), p. 6343-6353.
- [11] Tousizadeh M., Che H.S., Selvaraj J., Abd Rahim N., Ooi B.T., *Performance Comparison of Fault-Tolerant Three-Phase Induction Motor Drives Considering Current and Voltage Limits*, IEEE Transactions on Industrial Electronics, 2019, 66(4), p. 2639-2648.
- [12] Elbouchikhi E., Choqueuse V., Auger F., Benbouzid M.E., *Motor current signal analysis based on a matched subspace detector*, IEEE Transactions on Instrumentation and Measurement, 2017, 66(12), p. 3260-3270.
- [13] Li D.Z., Wang W., Ismail F., *A Spectrum Synch Technique for Induction Motor Health Condition Monitoring*, IEEE Transactions on Energy Conversion, 2015, 30(4), p. 1348-1355.
- [14] Corral-Hernandez J.A., Antonino-Daviu J.A., "*Thorough validation of a rotor fault diagnosis methodology in laboratory and field soft-started induction motors*," Chinese Journal of Electrical Engineering, 2018, 4(3), p. 66-72.
- [15] Xu Z., Hu C., Yang F., Kuo S.H., Goh C.K., Gupta A., Nadarajan S., *Data-Driven Inter-Turn Short Circuit Fault Detection in Induction Machines*, IEEE Access, 2017, 5, p. 25055-25068.
- [16] Keskes H., Braham A., *Recursive undecimated wavelet packet transform and DAG SVM for induction motor diagnosis*. IEEE Transactions on Industrial Informatics, 2015, 11(5), p. 1059-1066.
- [17] Faiz J., Ghorbanian V., Ebrahimi B.M., *EMD-Based Analysis of Industrial Induction Motors With Broken Rotor Bars for Identification of Operating Point at Different Supply Modes*, IEEE Transactions on Industrial Informatics, 2014, 10(2), p. 957-966.
- [18] Silva V.A.D., Pederiva R., *Fault detection in induction motors based on artificial intelligence*, In International Conference on Surveillance, 2013, 7, p. 1-15.
- [19] Konar P., Chattopadhyay P., *Bearing fault detection of induction motor using wavelet and Support Vector Machines (SVMs)*, Applied Soft Computing, 2011, 11(6), p. 4203-4211.
- [20] Lee C.Y., Wen M.S., Zhuo G.L., Le T.A., *Application of ANN in Induction-Motor Fault-Detection System Established with MRA and CFFS*. Mathematics, 2022, 10(13), p. 2250.
- [21] Lashkari N., Azgomi H.F., Poshtan J., Poshtan M., *Asynchronous motors fault detection using ANN and fuzzy logic methods*, IEEE Energy Conversion Congress and Exposition (ECCE), 2016, p. 1-5.
- [22] Patil, V. N., & Ingle, D. R. (2022). A Novel Approach for ABO Blood Group Prediction using Fingerprint through Optimized Convolutional Neural Network. International Journal of Intelligent Systems and Applications in Engineering, 10(1), 60–68. <https://doi.org/10.18201/ijisae.2022.268>
- [23] Refaat S.S., Abu-Rub H., Iqbal A., *ANN-based system for inter-turn stator winding fault tolerant DTC for induction motor drives*, 17th European Conference on Power Electronics and Applications (EPE'15 ECCE-Europe), 2015, p. 1-7.
- [24] M. J. Traum, J. Fiorentine. (2021). Rapid Evaluation On-Line Assessment of Student Learning Gains for Just-In-Time Course Modification. Journal of Online Engineering Education, 12(1), 06–13. Retrieved from <http://onlineengineeringeducation.com/index.php/joe/article/view/45>